Quantifying the impacts of groundwater abstraction on Ganges river water infiltration into shallow aquifers under the rapidly developing city of Patna, India

Chuanhe Lu [a,b,*], Laura A. Richards [a], George J.L. Wilson [a], Stefan Krause [c,d], Dan J. Lapworth [e], Daren C. Gooddy [e], Biswajit Chakravorty [f], David A. Polya [a], Vahid J. Niasar [g,**]

[a] *Department of Earth and Environmental Sciences and Williamson Research Centre for Molecular Environmental Science, The University of Manchester, Williamson Building, Oxford Road, Manchester M13 9PL, United Kingdom*
[b] *Cooling Circuit Department, Safety Research Division, Gesellschaft für Anlagen, und Reaktorsicherheit (GRS) gGmbH, Boltzmannstr. 14, 85748 Garching, Germany*
[c] *School of Geography, Earth and Environmental Sciences, University of Birmingham, Edgbaston, B15 2TT Birmingham, United Kingdom*
[d] *LEHNA, Laboratoire d'ecologie Des Hydrosystemes Naturels et Anthropises, University of Lyon, France*
[e] *British Geological Survey, Maclean Building, Wallingford, Oxfordshire OX10 8BB, United Kingdom*
[f] *National Institute of Hydrology, Phulwarisharif, 801505 Patna, Bihar, India*
[g] *Department of Chemical Engineering and Analytical Science, The University of Manchester, M13 9PL, Manchester, United Kingdom*

ARTICLE INFO

ABSTRACT

Study region: Patna is located on the southern bank of the River Ganges in Bihar, India. Rapid population growth over the past few decades has driven an increase in groundwater abstraction from aquifers under the city.

Study focus: This study explores the pumping-induced water exchange between the River Ganges and groundwater under transient conditions between 2009 and 2015, using a numerical simulation. The deterministic water exchange model within an uncertainty quantification was used to reveal the controlling factors affecting river water infiltration.

New hydrological insights for the region: Modelling reveals that under baseline (eno pumping) conditions, the dominant (~ 91% of the year) flow direction is from the aquifer to the river, which reverses (~ 9% of the year) when the river stage is high. When a municipal pumping well is implemented, river water infiltration into the aquifer increases to 68% of the year. The groundwater pumping rate is found to be the most important factor affecting the river water infiltration, whilst the groundwater table level is most sensitive to the well distance from the river, followed by pumping rate. Optimizing the location, depth and pumping rate of new wells in the area could mitigate fluvial contamination of the aquifer and help maintain groundwater levels.

* Corresponding author at: Department of Earth and Environmental Sciences and Williamson Research Centre for Molecular Environmental Science, The University of Manchester, Williamson Building, Oxford Road, Manchester M13 9PL, United Kingdom.
** Corresponding author.
E-mail addresses: chuanhe.lu@grs.de (C. Lu), vahid.niasar@manchester.ac.uk (V.J. Niasar).

1. Introduction

Climate change and population growth are causing an increasing reliance on groundwater across the globe. Groundwater is often assumed to be less susceptible to contamination from surface-derived contamination including pathogens and anthropogenic contaminants, although the potential risks associated with geogenic groundwater contaminants are often significant, like the dangerous concentrations of geogenic arsenic in groundwater because of changes of redox conditions etc. (Charlet and Polya, 2006; Ravenscroft et al., 2009; Richards et al., 2021, 2022; Smedley and Kinniburgh, 2002). The Ganges alluvial plain in India has a rapidly increasing population and a growing dependence on groundwater (Chatterjee et al., 2020; Duttagupta et al., 2020; Kumar et al., 2017; Saha et al., 2011). Increasing abstraction for agriculture and municipal water supplies can lower the groundwater level, which potentially changes geochemical conditions in the aquifer and the nature and extent of water exchange with the Ganges River (Brikowski et al., 2014; Das et al., 2021a, 2021b; de Graaf et al., 2019; Mukherjee et al., 2018). Beside the importance of managing geogenic contaminant risks related to intensive groundwater abstraction from interacting groundwater-river aquifers like the one at Patna, there is also an increased potential for groundwater contamination from anthropogenic contaminant sources in surface water through groundwater-surface water interactions, leading to groundwater quality deterioration (Duttagupta et al., 2020; Joekar-Niasar and Ataie-Ashtiani, 2009; Richards et al., 2021, 2022). Much research exists on flow of surface water to groundwater in response to municipal-scale groundwater abstraction (Goldschneider et al., 2007; Hubbs, 2006; Ray et al., 2003; Rosenberry and Healy, 2012; Schubert, 2006; Ulrich et al., 2015; Zhang et al., 2011), however, there is a lack of and need for this type of work in the context of the major river basins in the Indian subcontinent (van Geen et al., 2013; Wu et al., 2018; Das et al., 2021a, 2021b, 2018). Especially the groundwater table change, and the induced water exchange will affect the arsenic releasement in the aquifer, which is a major concern for the safe drinking water supply in Patna area (Richards et al., 2021, 2022).

The interactions between groundwater and rivers are of great importance in many growing cites in India that are situated on major rivers, e.g., Delhi, Kanpur, Varanasi and Patna, amongst others (Sandhu et al., 2011; Duttagupta et al., 2020). In such areas, most of the year the dominant groundwater flow direction is towards the river, contributing to baseflow. However, the dominant flow direction frequently reverses during the monsoon season when river water infiltrates into aquifers due to a higher river stage relative to hydraulic heads in adjacent groundwater systems (Chatterjee et al., 2020; Das et al., 2021a, 2021b; Shamsudduha et al., 2011).

Water exchange between river and groundwater is of key interest for understanding the potential implications of pumping on surface water infiltration and associated impacts on groundwater quality. Hydraulic head gradients along the river-alluvium boundary drive the exchange between river and groundwater (Boano et al., 2010, 2014, Cardenas, 2009a,b; Gomez-Velez et al., 2012; Gomez-Velez and Harvey, 2014; Jasechko et al., 2021; Kiel and Cardenas, 2014; Krause et al., 2011; Magliozzi et al., 2018; Munz et al., 2011; Song et al., 2020; Wu et al., 2018). As surface water infiltrates the groundwater system, it interacts with minerals and microbes of the ambient sediment. This can cause changes to the redox conditions, dissolution/precipitation processes and other biogeochemical reactions, leading to changes in both water chemistry and biological activity in the aquifer (Battin et al., 2008; Boano et al., 2010, 2014; Gomez-Velez and Harvey, 2014; Johannesson et al., 2019; Mulholland et al., 2008; Saunders et al., 2005; Wallis et al., 2020). Some of this infiltrated water may eventually return to the river, particularly in non-monsoonal seasons when the directions of hydraulic head gradients in the aquifer tend to reverse (Wroblicky et al., 1998).

Quantifying the extent of groundwater-river water exchange and residence time is very important for understanding how groundwater quality and quantity may change along dominant groundwater flow paths (Ascott et al., 2021; Boano et al., 2014; Goldschneider et al., 2007; Hubbs, 2006; Kiel and Cardenas, 2014; Krause et al., 2011; Mehmood et al., 2022; Ray et al., 2003; Rosenberry and Healy, 2012; Schubert, 2006; Song et al., 2020; Trauth et al., 2018; Ulrich et al., 2015). The water flow between a river and the aquifer is a dynamic process not only because of changing river levels and potentially changing groundwater levels, but also potentially changing groundwater abstraction and pumping regimes (Chow et al., 2020; Rizzo et al., 2020; Song et al., 2020). The residence times for river water entering the aquifer can span a broad range, from days to decades (Boano et al., 2014; Song et al., 2020; Wörman et al., 2007). There are many factors controlling the water exchange and the distribution of infiltrated water, including the depth to the groundwater table and the irregular planform morphology of the river (Wroblicky et al., 1998), the sinuosity of the planform (Cardenas, 2009b), management of surface water flow using barrages built across the river (Lapworth et al., 2021), spatial patterns of permeability in riverbed sediments (Boano et al., 2007; Cardenas et al., 2004; Chow et al., 2020; Jasechko et al., 2021; Marion et al., 2008; Mehmood et al., 2022; Salehin et al., 2004; Sawyer and Cardenas, 2009; Stonedahl et al., 2018; Vaux, 1968) and temporal evolution driven by a single-peak discharge event (Ascott et al., 2016; Singh et al., 2020; Wu et al., 2018, 2020). However, some of these studies have not considered the influence of groundwater abstraction by pumping on these interactions. Some studies considered this effect, but the groundwater abstraction is generally treated simplistically as a sink/source term in the system causing water drawdown in the dry season for irrigation or municipal purposes (Boano et al., 2014; Zhang et al., 2011, 2017).

Numerical models have been applied successfully across different spatial and temporal scales to quantify lateral exchange fluxes between groundwater and rivers (Cardenas, 2009a,b; Kiel and Cardenas, 2014; Mehmood et al., 2022; Munz et al., 2011; Rosenberry and Healy, 2012; Sawyer and Cardenas, 2009; Su et al., 2007). Chow et al. (2020) developed a highly-parameterized model to evaluate the trade-offs between intrinsic and epistemic model errors when choosing between homogeneous and highly complex subsurface parameter structures to simulate hyporheic exchange in the Steinlach River test site in Germany. Numerical models have been shown to be a fast and efficient way to quantify the uncertainty of controlling factors for water exchange in complex regimes (Boano et al., 2007, 2010, 2013, 2017; Marzadri et al., 2016; Mehmood et al., 2022; Song et al., 2020; Trauth and Fleckenstein, 2017; Ward et al., 2017; Wu et al., 2018).

Here, we develop a 2D numerical model for quantifying River Ganges - groundwater interactions in the growing city of Patna, Bihar (India). Observations made along a river-groundwater transect in the study area enable a detailed assessment of the impacts of rapidly

growing urban water demand on river-groundwater interactions to be made. The focus of our study is to determine to what extent groundwater pumping, from modelled municipal drinking water supply boreholes, can impact river-groundwater interactions. After calibrating the model with data from CGWB (2015) and evaluating the model with the available groundwater level observations, we consider several plausible scenarios of groundwater abstraction regimes under transient conditions (for both river water level and rainfall in the region) to: (1) quantify the extent of expected water exchange between the River Ganges and groundwater under transient conditions, (2) estimate the spatial distribution and residence time of river water infiltration in the shallow aquifers underlying Patna; (3) characterize the impact of monsoon on the water exchange; and (4) identify the critical factors influencing the river-groundwater exchange due to pumping with a global sensitivity analysis. The findings of this study can contribute to baseline understanding to potentially inform groundwater management practice in Patna and other similar rapidly expanding urban areas, where the groundwater quality may be deteriorated by surface water sources through natural or anthropogenic groundwater-surface water interactions (Duttagupta et al., 2020; Joekar-Niasar and Ataie-Ashtiani, 2009; Richards et al., 2021).

2. Methodology

2.1. Case study

Patna is located on the southern bank of the River Ganges in Bihar, India (Fig. 1). Over the past three decades, there has been a substantial growth of the urban population as well as an expansion of industrial/commercial activities with a concomitant increasing demand for water, resulting in increased groundwater abstraction (Alakshendra, 2019; Saha et al., 2014). The area has a sub-tropical to sub-humid climate with a monsoon season from June to September, which accounts ~ 82% of average annual rainfall (CGWB, 2015). July and August are the wettest months and in the past decade accounted for ~ 51% of mean annual rainfall (Saha et al., 2014).

The Middle Ganges Plain in Patna is underlain by two major Quaternary aquifers within a depth of 300 m below ground level, separated by a 15 – 32 m thick clay/sandy clay layer (Fig. 1) (Saha et al., 2014). A pervasive layer of clay mixed sand constitutes the top aquitard of the succession. The presence of Kankar nodules (concretions of lime) and fine sand makes this clay layer semi-permeable. Underneath and near the Ganges, this clay/sand clay layer consists of several thinner clay lens with sand. The Ganges is the groundwater outflow boundary according to the local hydrogeological conditions (CGWB, 2015; Das, 2021a, 2021b), with the net flow of groundwater from the south west to north east towards the Ganges in Patna (CGWB, 2015).
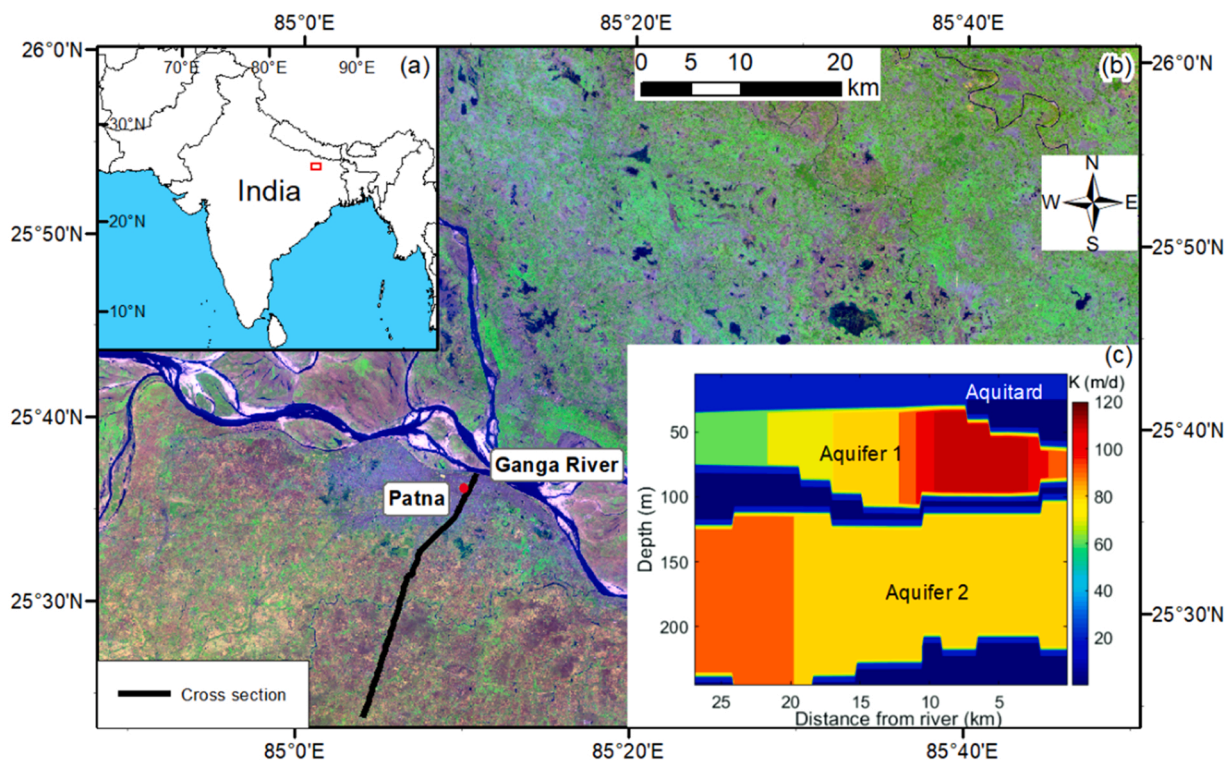

Fig. 1. Study area (a, b) with false colour normalized difference vegetation index (NDVI) for land use (b). In the land use map (b), blue represents water bodies, green - trees and crops, grey - urban buildings and brown - bare land cover. The USGS Landsat 8 OLI/TIRS surface reflectance data for zone (140 042) in December 2019 is used to classify the land use type in the study area (https://earthexplorer.usgs.gov/). Inset figure (c) shows the 2D hydraulic conductivity (m/s) distribution, based on CGWB (2015), along the cross section (black line in the map). The red point close to the cross section is where the observation data will be used for validation of the numerical base model.

2.2. Hydrological parameterization

Subsurface layers were parameterized for the purposes of numerical modelling (the modelling framework is described in Section 2.3). The layer stratification and thickness were interpolated on the basis of previous geophysical logging reports (CGWB, 2015) in some locations near a cross section running roughly perpendicular from the Ganges inland from Patna (Fig. 1b). Pumping test data of CGWB wells (CGWB, 2015) indicate that the transmissivity of the aquifers ranges between ∼ 4900 and 16000 m^2/day with a mean of ∼ 8300 m^2/day. The specific capacity of the wells ranges from ∼ 56 – 100 m^3/hr/m and the mean hydraulic conductivity (K) has been reported ∼ 87 m/day, corresponding to that of coarse sand and coarse sand mixed with gravel. Hydraulic conductivity data obtained from pumping tests conducted by CGWB (2015) was utilized through interpolation. In terms of hydraulic conductivity anisotropy, vertical hydraulic conductivity was assumed to be 10% of the horizontal hydraulic conductivity (CGWB, 2015). The hydraulic conductivity of the top aquitard layer (thickness 28 – 60 m) has been estimated through grain size analysis (CGWB, 2015). The range of hydraulic conductivity for this layer varies from 5 m/day to 20 m/day. The hydraulic conductivity of the first aquifer (Aquifer 1, lying between 40 and 110 m) has been estimated to between ∼ 60 and 120 m/day; and the hydraulic conductivity of the deeper aquifer system (Aquifer 2, lying below ∼ 120 −130 m depth) has been estimated to be between ∼ 82 and 92 m/day (CGWB, 2015). Groundwater in the deeper aquifer occurs under semi-confined to confined conditions due to the relatively poor hydraulic conductivity of the middle clay between Aquifer 1 and Aquifer 2 (5 m/day). Below Aquifer 2 it is assumed to be impermeable (hydraulic conductivity ∼ 7.2 ×10^{-3} – 4.7 ×10^{-2} m/day) (CGWB, 2015).

The porosity of various major layers has been estimated using the equation given by Vukovic and Soro (1992):

$$n = 0.255(1 + 0.83^{\frac{d_{60}}{d_{10}}}) \qquad (1)$$

where d$_{60}$ is the 40% retained grain size and d$_{10}$ is the 90% retained grain size. The calculated porosities are as follows: 0.01 for clay layer, top 0.35 for aquitard layer (with range 0.34 – 0.37), 0.38 for the middle aquifer (Aquifer 1) (with range 0.36 – 0.4), and 0.35 for the deep aquifer (Aquifer 2) (with range 0.33 – 0.40) (CGWB, 2015). Porosity estimates could be improved in future models if direct corresponding measurements were systematically made with depth across the modelled transect, however this data was not available at this time of this study. The assumed structure of the subsurface may not capture local heterogeneity such as the existence of unknown clay lenses or high permeable lenses, especially as the detailed 3D substructure of the modelled transect and wider study area is not available (CGWB, 2015; Saha et al., 2014).

2.3. Modelling framework

A two-dimensional domain was established to represent the ∼ 27 km cross section oriented approximately perpendicular to the river along expected dominant groundwater flow paths (Fig. 1b). This cross section starts from the river and goes in the direction of southwest. It passes through the east Patna urban area and crosses the south farming land until 27 km faraway from Ganges, in which the river is the outflow boundary and the location around 27 km is near the local surface water divide based on the GIS data analysis. It was selected because of the available geophysical survey profile, which was nearby and parallel to this cross section (CGWB, 2015). It is also because that groundwater geochemical measurement was performed in several locations at this cross section, along which the current work findings will be used for next step geogenic contamination numerical simulation (Richards et al., 2021). We used this cross section to estimate the extent of groundwater-river water exchange under natural transient conditions (e.g., as influenced by seasonally variable river water levels and precipitation). The 27-km-long cross section is 250 m deep and 50 m wide, which covers the
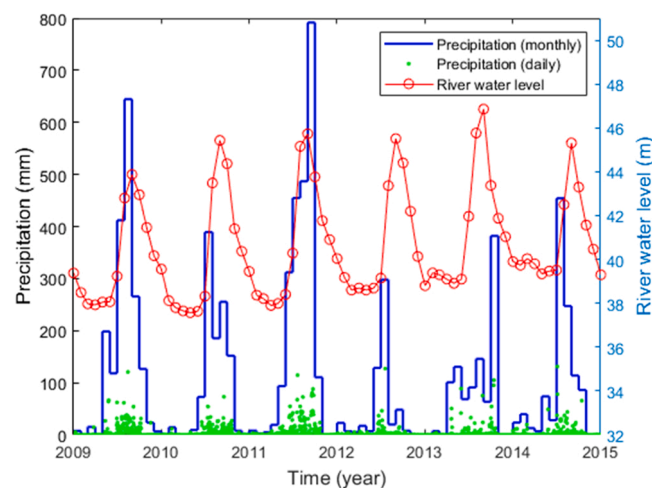

Fig. 2. Average monthly (blue line) and daily (green points) precipitation in Patna (left Y-axis) (Worldweatheronline, 2021) and Ganges River water level near Patna (Coss et al., 2020) (right Y-axis) from January 2009 to December 2014.

effect radius of the pumping wells. It was discretized into 4988 grid cells with variable horizontal discretization length ranging from 0.625 m (near the river) to 1000 m (in the south boundary) and variable vertical discretization length ranging from 0.625 m near the surface to 10 m at the bottom depths. In total there are 172 columns and 29 layers for the discretization.

The River package in Modflow 6 (Hughes et al., 2017) is used for the Gangetic model. The conductance of the river boundary is 1000 m^2/day assuming that the hydraulic conductivity of the riverbed is 0.1 m/day, with a thickness of 0.5 m. To establish boundary conditions for the river, a time series of Ganges water level data was provided by NASA, viz. Pre SWOT Hydrology GRRATS Virtual Station River Heights (Coss et al., 2020). The rainfall is the major water source term in the area. Average precipitation values for Patna for the January 2009 to December 2014 period were used to establish the groundwater flow model as this represents a recent continuous record (Worldweatheronline, 2021) (Fig. 2). The ground surface elevation analysis also shows that the surface water runoff accumulates and flows mostly in direction to east and into the downstream of Ganges in Patna (https://earthexplorer.usgs.gov/), only the surface runoff in a small area at north-west part of Patna will flows directly to the Ganges at Patna. The rainfall infiltration ratio was calibrated to fit the groundwater head distribution map of Patna (CGWB, 2015). Both of the rainfall rate and infiltration rate were assumed to be universal along the cross section.

The Processing Modflow platform (Chiang and Kinzelbach, 2003) was used to simulate water flow through Modflow (Hughes et al., 2017) and conservative tracer transport in the aquifer through MT3D (Bedekar et al., 2016), and exchange with river water. A transient model was set up for 6 years using existing rainfall and river level data. This 6-year time period was restricted by availability of river water level data (Coss et al., 2020). We also ran a steady state model for the initial groundwater distribution. Conservative tracers were virtually added in the river to track water exchange between the river and aquifer, using a molecular diffusion coefficient of 8.64×10^{-5} m^2/day and a horizontal dispersivity of 5 mm, based on the reported aquifer grain size distribution (CGWB, 2015). The ratio between tracer concentration in the pumping well and initial concentration in the river ($C/C_0 = 0.1$ and 0.01 respectively) were used to identify the modelled proportion of river source water in the pumped water.

The transient model without introducing pumping schemes was performed as an initial base run to determine the extent of groundwater-surface water exchange, including the effect of the annual monsoon. This base model was validated with the groundwater table data observed at Kankerbagh, Patna. Two models considering the impact of pumping scenarios for municipal (typically targeting deeper groundwater from Aquifer 2 with depth > 100 m) and agricultural purposes (typically targeting shallow groundwater in aquitard with depth < 50 m) were then run. In the first scenario, a new planned municipal purpose pumping well is located 1 km from the river with a depth of 175 m (in Aquifer 2), and a high pumping rate of 2000 m^3/day (the pumping rate of the municipal purpose well in Patna is between 1875 and 2500 m^3/day) (CGWG, 2015). In the second scenario, a new planned irrigation purpose pumping well is located 1 km from the river with a depth of 45 m (in aquitard) and a pumping rate of 1000 m^3/day. Together with the base simulation, the changes in residence time of water from the river were assessed. Two alternative models were run to estimate the effect of multiple wells on river and aquifer water exchange. The pumping rates of two pumping wells were given as half of the rate of the single well scenario. There was one well located also 1 km from the river, and another well located at 2 km and 0.5 km from the river in the different two well scenarios, respectively. Finally, to investigate the sensitivity of well parameters affecting the water exchange dynamics, we used the PSUADE (Problem Solving environment for Uncertainty Analysis and Design Exploration) code (Tong, 2017) with the PMWIN to conduct the uncertainty quantification (UQ) analyses. PSUADE is a software package for various UQ activities, such as uncertainty assessment, global sensitivity analysis, risk analysis, design optimization and parameter identification.

Three major factors were considered to simulate the effect of groundwater pumping on the water exchange between the aquifer and river: pumping rate, well distance from the river and well depth. The daily pumping rate of the wells for drinking water supply in Patna are typically between 1875 and 2500 m^3/day (calculated using estimated pumping rates and daily hours of usage) (CGWB, 2015). The following ranges were used for sensitivity analysis: 1800 – 2500 m^3/day for pumping rates; 2 – 3000 m perpendicular distance from the river for well locations; and 15 – 225 m for well depth. One pumping well was implemented for the sensitivity analysis given that total pumping rate is a more influential parameter on water exchange in comparison to well location or number of wells. A Latin hypercube method (Tong, 2017) was used to produce 200 simulations with these different factors randomly distributed within the ranges indicated above. The sensitivity of infiltrated river water extent area and the groundwater drawdown to the 3 factors were assessed. In order to prevent the observation point from being close to the well in one model and far from the well in the other model, the water drawdown at 25 km, which is far from the pumping well in all models, was selected for the final sensitivity analysis.

To determine the modelled destination and the travel times of the infiltrated river water, individual conservative particles, which will transport together with water, were considered. Particles were released virtually into the river. They were traced on their way into the aquifer, when the river water level was relatively high, and then out of the aquifer, when the hydraulic head in the aquifer was relatively higher than that of the river. The pathway of a particle was observed with time from a starting point.

Particle transport velocities were described as $\frac{dx}{dt} = v(x(t))$, with the position of the particle $x(t)$ at a specific time t given by the equation:

$$x(t) = x_0 + \int_0^t v(x(\hat{t}))d\hat{t} \qquad (2)$$

where x_0 is the initial position of the particle and $v(x(t))$ is the seepage velocity at a particular location $x(t)$.

The seepage velocity was used to determine the travel time, τ of a particle. This was integrated (Eq. 3) over the travel path of a particle, beginning at its starting point x_0 and ending at an observation point x:

$$\tau(x) = \int_{x_0}^{x} \frac{dX}{\|v(X)\|} \tag{3}$$

A Matlab code was developed to simulate the particle tracking process. The seepage velocity was updated every time step based on the time-dependent hydraulic head distribution.

3. Results and discussion

3.1. Model validation

For the base scenario model, the rainfall infiltration ratio was calibrated with the groundwater hydraulic head distribution data in CGWB (2015). Therefore, the initial hydraulic head distribution is consistent to those reported in CGWB (2015). CGWB (2015) reported also water table depth observation data collected monthly from November of 2011 to June of 2014 in Patna area, in which the well in Kankerbagh (around 3 km from the river) is 500 m away from the modelled cross section (Fig. 1b). We used these data for the model validation (Fig. 3) and the comparison show that the results of basic scenario model match the seasonal variability in observed groundwater levels.

The differences between the simulated and observed water table depth are in reasonable range (Fig. 3a). The mean error between calculated and observed values is 0.03, and the root mean squared error is 0.85 (Fig. 3b). The numerical model captured the observed water table depth evolution trend: it increases during pre-monsoon season, decreases after the onset of the monsoon and then increases again in the post-monsoon season. The difference is relatively bigger at maxima and minima of the evolution curve (Fig. 3a); this is likely because a uniform precipitation rate and rainfall infiltration rate were used along the whole cross section. The heterogeneity of the aquifer's physical properties is another possible reason for the smooth numerical evolution curve. A slow infiltration of rainfall at the observation location will delay the groundwater table response to rainwater, whilst also reducing variability exhibited in the water table evolution curve. Therefore, detailed measurements of the heterogeneous distribution of porosity would improve future simulations. The variable precipitation rate and rainfall infiltration rate in different parts of the cross section, depending on in situ measurement and observation data, would improve the delineation of the source term in the model. Seasonal tracer tests near the river would help also in model validation and identifying target areas for more detailed modelling.

3.2. Surface water-groundwater interactions under transient conditions

Generally, the Ganges gains flow from groundwater in Patna (Fig. 4), because the alluvial plain has a higher piezometric head compared to the river water level. The groundwater flows northward, from the south of Patna to the river (Fig. S1). When the monsoon season starts, typically in July, precipitation increases, as well as the water level in the Ganges River. Near the river, the hydraulic head in the aquifer responds to the river water quickly and has a similar temporal pattern to that of the river water level (Fig. 4 and Fig. S1). The largest increases in hydraulic head in the river drive water flow from the river into the aquifer (Fig. S1 and the yellow-colored zone in Fig. 4).

The numerical simulation shows that if river water infiltration occurs, this mostly happens in late July, August and early September,
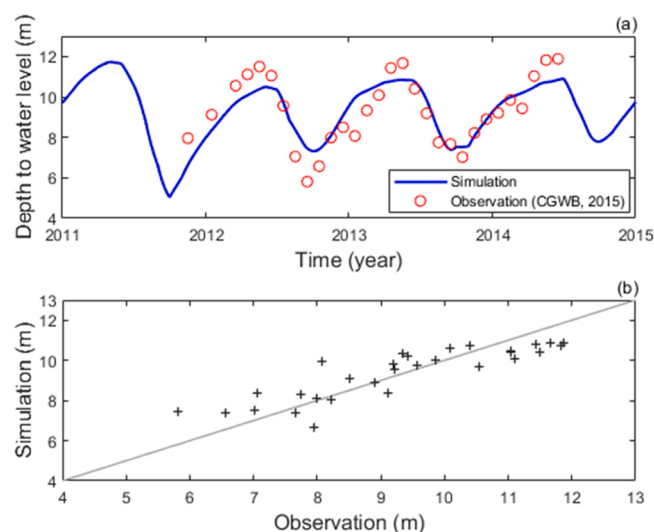

Fig. 3. Depth to water level comparison between simulation results at location 3 km from the river and observation data (monthly data from November of 2011 to June of 2014) at Kankerbagh, Patna (500 m away from the cross section and 3 km from the river): (a) depth to water table evolution from 2011 to 2014; (b) simulated depth to water table versus observation data (CGWB, 2015).
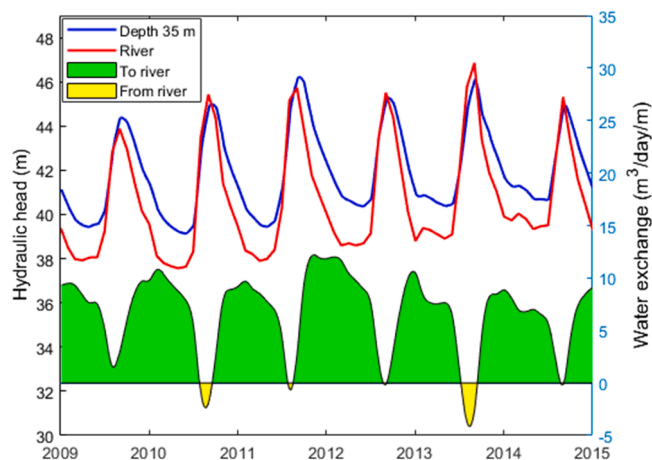
Fig. 4. Calculated hydraulic head in the aquitard at Patna (35 m depth and 75 m away from the river) (left Y-axis) and water level in the River Ganges, together with modelled water exchange between the river and aquifer (right Y-axis, the unit means m³/day along 1 m length of the river) from 2009 to 2015. Positive values, shown in green, indicate groundwater flow to the river, negative values, shown in yellow, indicate water flow from the river into aquifer.

depending on the annually-dependent onset of the monsoon period and river water level (Fig. 4). During the monsoonal period, the groundwater hydraulic head in the aquifer increases near the river and the location of the minimum head values moves to 2 – 5 km away from the river, extending to the south side of the urban area of Patna city. In late September, even though the river water level is still high, the accumulation of rainwater since June causes the accumulated hydraulic head in the south zone to become higher, so the direction of groundwater flow changes back to from south to north (i.e., towards the river) again in September (see Fig. S1). On average, the Ganges River becomes a source term for the groundwater just 9% of the year (around 33 days with range 0 – 68 days) for the selected cross section.

For the simulation period from 2009 to 2014, when the river water levels in 2010 and 2013 were still higher in August and September because of the relative high rainfall in the upstream region of Ganges, the rainfall in Patna were lower, so the river water moved into the aquifer for longer periods in those years (Fig. 2 and Fig. 4). For example, there were ~ 68 days in 2013 with river water infiltration, starting relatively early at the beginning of July. However, in 2009, the river water level was relatively low, and the rainfall was higher than average; in this year there was no river water movement into the aquifer. The river water level in 2011 was relatively high, but the precipitation in 2011 at Patna was the highest in 6 years. since most of the surface water runoff at Patna region goes to the east direction and it flows finally to the downstream of Ganges, so the local rainfall would result in greater recharge to groundwater, but less amount direct to the Ganges in the north of Patna. Then, comparing with other year, the river infiltration time was short (~ 28 days starting mid-July) and the rate is lower compared to that in years of 2010 and 2013. The effect of high and prolonged precipitation in 2011, causing river infiltration in 2012 to have a very short duration (~ 22 days, starting at the beginning of
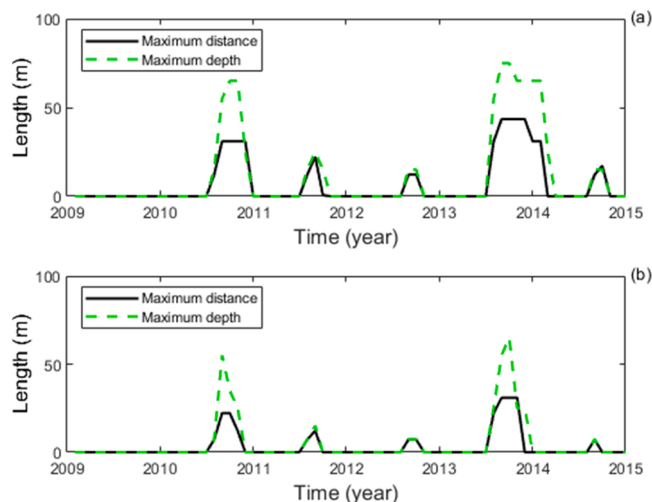

Fig. 5. Modelled spread of a conservative tracer plume, defined based on two threshold values: $C/C_0 > 0.01$ (a), $C/C_0 > 0.1$ (b). The black solid line shows the plume maximum distance from river, and green dash line shows the maximum depth of the plume.

August) and a lower rate of flow. In 2014, both the water level and rainfall in monsoon are low, the river water infiltration started on middle of August and only lasted ~ 19 days (Fig. 4).

The CGWB (2015) reports have shown that the groundwater table reached a minimum before the monsoon in 2014 due to low precipitation and continuing groundwater abstraction, especially in urban areas, which may cause river water inflow in some part of Patna, noting the river water level is also relatively low pre-monsoon (CGWB, 2015). Das et al. (2021a) showed that contribution of groundwater in Ganges baseflow is estimated to be the highest during dry season whereas during monsoon the flow direction also reverses in Varanasi.

River water and hence tracer infiltration varies considerably between years with the volumes particularly small in 2011, 2012 and 2014 (Fig. 5). There is a clear plume of the conservative tracer distributed in the shallow depth (< 75 m) for short time (~ 28, 22 and 18 days for 2011, 2012 and 2014 respectively). The plume of the tracer extends horizontally and vertically with time. The maximum distance and maximum depth of tracer plume are larger when the infiltration rate of river water is highest (years 2010 and 2013 in Fig. 5). The tracer plume reaches the maximum extent at the middle of September. Thereafter, because the water flux direction reverses, the infiltrated tracers are transported towards the river and the plume shrinks. When the flow from the river to aquifer is small (2011, 2012 and 2014), the infiltrated tracer leaves the aquifer earlier and almost completely disappears at the end of the year. When the flow of water from the river is high in the monsoon season, the tracer needs a longer time to transport out of the aquifer and some tracer lasts until the following year (Fig. 5a with $C/C_0 > 0.01$ in year 2013). The maximum residence time of the tracers in aquifer varied between 1 and 7 months. A similar pattern of tracer transport is repeated every year with a different plume extent due to the variation of rainfall and river water level. The maximum lateral extent of the plume is small, reaching 75 m in years with higher rates of river water to aquifer flow, whilst the maximum modelled depth of the plume in the aquifer was 45 m (Fig. 5a with $C/C_0 > 0.01$ in year 2013).

If the plume extent is instead estimated using the cut-off concentration $C/C_0 > 0.1$, the modelled plume dissipates faster and moves out of the aquifer around 1.5 – 3 months after the start of the monsoon (Fig. 5b and Fig. S2). As a result, the majority of tracer moves in and out with the water exchange between river and aquifer, but there is still a small proportion of the tracer that remains in the aquifer for a much longer time.

3.3. Effect of pumping on the river-aquifer water exchange

When there is a pumping well located 1 km from the river, it significantly effects the water exchange between the river and aquifer (Fig. 6), the maximum flux rate towards river decreases around 80% for the scenario with municipal purpose well, and around 40% for the scenario with irrigation purpose well. The decrease of flux rate towards river in scenario with municipal purpose well is around double of that in scenario with irrigation purpose well. Pumping reduces the rate of groundwater transport to river, with higher pumping rates, steeper decreases of water exchange rate and an earlier reversal of water exchange direction. In the scenario with shallow irrigation purpose pumping well (lower pumping rate), the rate of groundwater flow to the river decreases, and the river water infiltration occurs in the first year, which is not seen in the base simulation. The rate of river water infiltration increases compared to base simulation. However, during most of the time in the year, the water exchange direction is still from aquifer into river. The river water infiltration rate is around 1.5, 1.7, 3.4, 0.94 and 2.5 times of that of base model in year 2010, 2011, 2012, 2013 and 2014, respectively. And on average, the time of river water infiltration increases to 23% of the year (around 84 days with range 62 −110 days). In the scenario with the municipal purpose well (higher pumping rate), the river water infiltration lasts for a much longer period
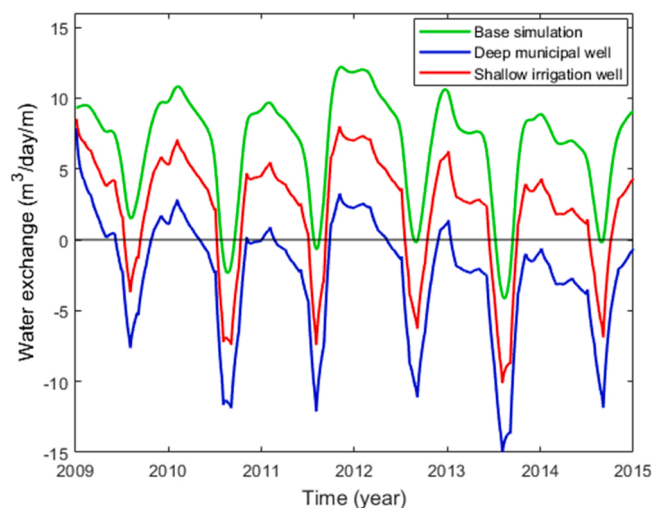

Fig. 6. Comparison of water exchange between river and aquifer with different pumping scheme: base run (green line) without planned pumping well, the run with the planned deep well (blue line, 1 km from the river, depth 175 m, pumping rate 2000 m³/day) and the run with the planned shallow well (red line, 1 km from the river, depth 45 m, pumping rate 1000 m³/day).

of time and at a higher rate (blue line in Fig. 6). The increment of river water infiltration rate, compared to the base model, is double of that of scenario with irrigation purpose well. The river water infiltration continues for most of the year and there even was no apparent groundwater flow towards the river in the last year. The time of river water infiltration increases to 68% of the year (around 253 days with range $140 - 365$ days). However, the evolution pattern of the river water plume is still affected by the transient conditions.

Since there is less groundwater flowing to the river in the scenario with municipal pumping well, there is more tracer continuing into the aquifer, and the tracer plume expands in distance and depth (Figs. 7 and 8). After 6 years, the plume extends more than 500 m from the river, reaches 180 m depth and reaches a state where the plume does not recede further. For the scenario with irrigation pumping well, the maximum depth reaches to 110 m, which is caused by the vertical flow downward close to the river, but most of the plume stays not beyond depth 60 m. This demonstrates that if a new pumping well is installed, the abstraction rate and location should be selected carefully to avoid contamination from river water.

3.4. Transport time of water from the river to the aquifer

Fig. 9 shows the transport time of a particle to the maximum distance in the aquifer and the total transport time of the particle in the aquifer for the base simulation and scenario with a shallow irrigation well. In the base run, there was no river water infiltration in 2009, and so there are no data shown. In 2010 and 2013, the river water infiltration lasted a longer time with relatively high rates (Fig. 6), the particle transports for a longer time to the maximum distance (56 and 68 days for 2010 and 2013, respectively). The travel times to the maximum distance are less than 1 month (28, 22 and 22 days) in 2011, 2012 and 2014, respectively. In the scenario with the shallow irrigation well, in which the river water infiltration time is longer and the rate is higher (Fig. 6), the particle travels for a much longer time. After more than 2 months, the particle reaches the maximum distance in each year (62, 68, 89 and 83 days in 2009, 2011, 2012 and 2014, respectively). In 2010 and 2013, the particle travels for more than 3 months to the maximum distance (95 and 110 days, respectively). When the flow direction of groundwater changes, the particle starts moving back towards the river. For the base simulation, the particles travel for a shorter time leaving the aquifer because of the higher flow rates into the river (34, 21, 15, 42 and 14 days, respectively from 2010 to 2014). In terms of total travel time in the aquifer, the maximum particle residence times in the aquifer are 90, 49, 37, 110 and 36 days, in 2010 – 2014, respectively.

In the scenario with the shallow irrigation well, in contrast, the particle starts moving back to the river relatively slowly because the water flow rates are lower compared to those during the infiltration period in 2010 and 2013 (Fig. 6). Thereafter, the particle travel time to leave the aquifer is much longer (109 and 248 days in 2010 and 2013, respectively), remaining in the aquifer through the year. In 2009, 2011 and 2012, the flow rates to the river are still lower than those in the infiltration period, but the difference is not substantial. It takes 52, 50 and 74 days for the particle to leave the aquifer. In 2013, the maximum residence time in the aquifer is about one year (358 days). The particle transported into the aquifer in 2014 stayed in the aquifer until the end of the year (end of the simulation), and so the total transport time is not shown here. Therefore, the pollutants carried by the river water plume will be transported deeper and for a longer distance into the aquifer when a new pumping well is made operational. Additionally, the plume will stay a longer time in the aquifer and may not ultimately be transported out of the aquifer (Figs. 7, 9 and Fig. S3).
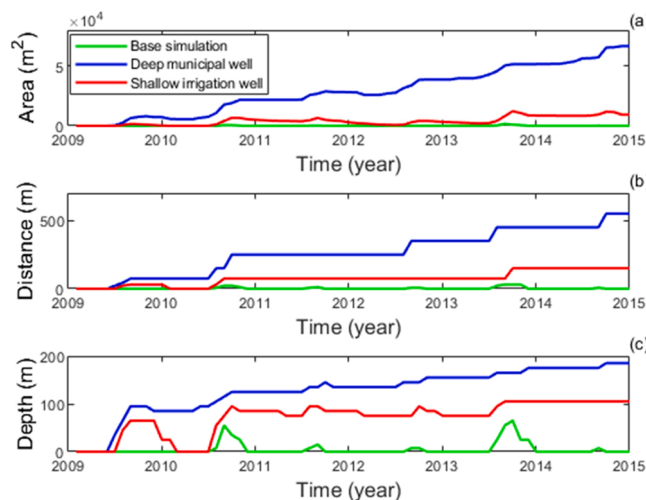

Fig. 7. Comparison of characteristics of a modelled conservative tracer plume ($C/C_0 > 0.01$) of the two pumping scenarios with the base simulation: The plume covered area (a); the maximum plume extent from the river (b); the maximum depth of plume in aquifer (c). Green line represents the base simulation (no well), blue line represents the scenario with a deep municipal pumping well (rate of 2000 m^3/day; depth of 175 m) and the red line represents the scenario with a shallow irrigation pumping well (rate of 1000 m^3/day; depth of 45 m).
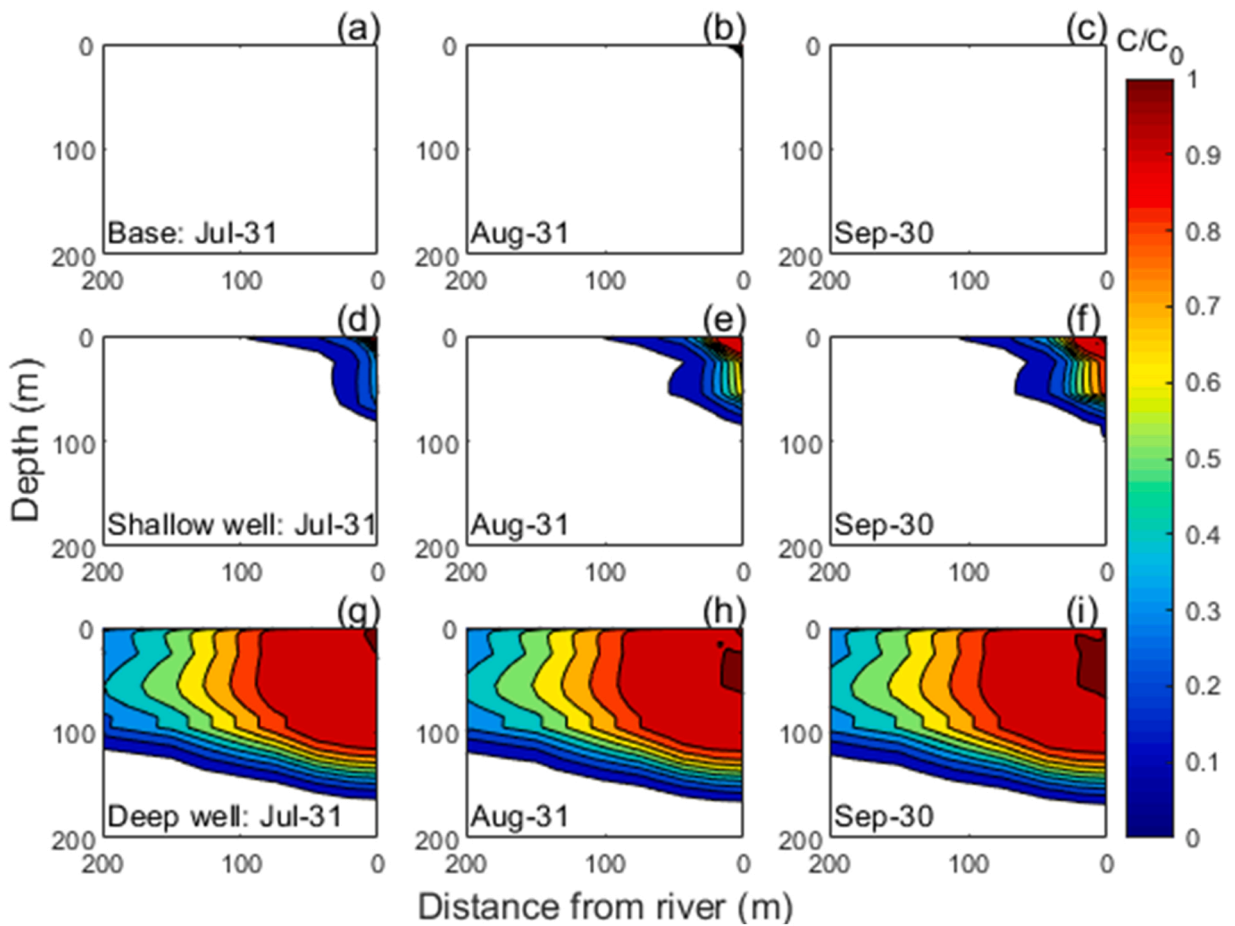
Fig. 8. Modelled distribution and evolution of conservative tracers ($C/C_0 > 0.1$) at 2014. Top (a, b and c): base simulation (no well); middle (d, e and f): simulation with a shallow well (rate of 1000 m^3/day; depth of 45 m); bottom (g, h and i): simulation with a deep well (rate of 2000 m^3/day; depth of 175 m). The three subplots on the left side (a, d and g) are results at July 31; the three subplots in the middle column (b, e and h) are results at August 31; the three subplots on the right side (c, f and i) are results at September 30.

3.5. Effect of multiple pumping wells on the river-aquifer water exchange

The effects of multiple pumping wells on the river-aquifer water exchange and water drawdown were evaluated before a sensitivity analysis based on the single pumping well was carried out. The scenario with deep municipal well was used for comparison. Well locations at 0.5, 1 and 2 km were selected because these locations are close to the river and in the sub urban area, the groundwater abstraction is needed. The comparison shows that, there are very small differences (< 0.4 m^3/day/m) for the water exchange between river and aquifer after the groundwater abstraction commences, but the three models have the similar water exchange rate after six months (Fig. 10a). The comparison of hydraulic head indicates the differences are obvious when the water head is high during monsoon season and low before the monsoon arrives (Fig. 10b). The total pumping rate of multiple pumping wells is important for the water exchange between river and aquifer, whilst the effect of well location is insignificant. The well location does affect the groundwater head distribution.

3.6. Sensitivity analysis

The results (the river infiltration flux area, and the water drawdown observation at location 25 km from the river) from the 200 successful realizations (Fig. 11) with different pumping rate and well location setups were used for a Sobol sensitivity analysis, a form of global sensitivity analysis (Sobol, 2001), to then identify, using PSUADE, which parameters are most important (Fig. 12).

The pumping rate is the dominant factor controlling the extent of the conservative tracer plume (Figs. 11 and 12). When the pumping rate is high, there is more water infiltration from the river, and this is widely dispersed into the aquifer (Fig. 11a). The flux area of river infiltration shows a clear relationship with the pumping rate (except the wells very close to the river). The flux area increases from around 2.8×10^4 m^2 to around 6×10^4 m^2 when the pumping rate increases from 1800 to 2400 m^3/day, the area doubles which the pumping rate increases only one third. However, the groundwater table change at $\sim$ 25 km shows a relationship
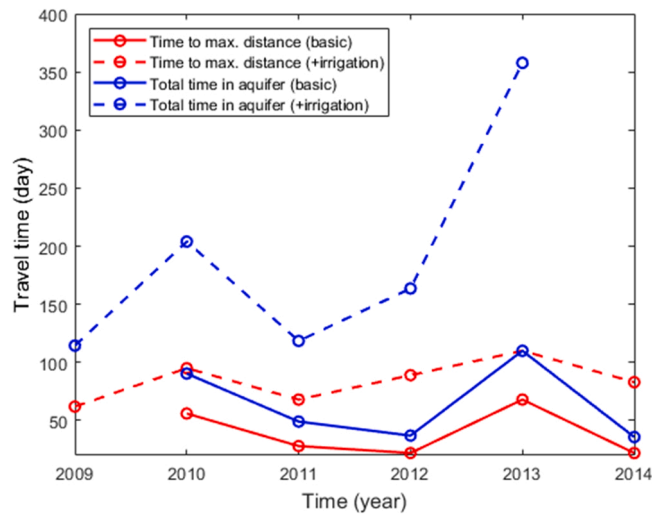
Fig. 9. Estimated travel time (days) of water from river in the aquifer (starts with the beginning of river water infiltration) for the basic simulation (solid line) and the scenario with a shallow irrigation well (dashed line). Red lines indicate the transport time to the maximum distance from the river, blue lines indicate the total transport time in the aquifer (i.e. the travel time between entering and leaving the aquifer). There is no river water infiltration in 2009 for the basic simulation (Figs. 4, 5, 6, 7).
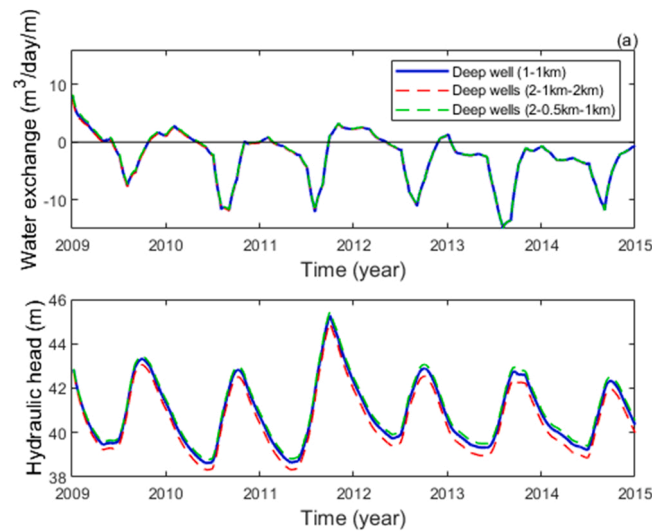

Fig. 10. Comparison of modelled water exchange between the river and aquifer (Fig. 10a: the unit means m³/day along 1 m length of the river) and hydraulic heads at location with depth 45 m and distance 3 km from the river (Fig. 10b) from 2009 to 2015 for different (with depth 175 m) pumping well setups: 1 pumping well with pumping rate 2000 m³/day and 1 km from the river (blue solid line); 2 pumping wells both with pumping rate 1000 m³/day, one is 1 km and another is 2 km from the river (red dash line); 2 pumping wells both with pumping rate 1000 m³/day, one is 1 km and another is 0.5 km from the river (green dash line). Positive values indicate groundwater flow to the river, negative values indicate water flow from the river into aquifer.

with the well distance from the river clearly, with the water table decreasing more when the well is far from the river (Fig. 11e). When the well is located far away from the river in the southern part of the cross section, pumping will have a greater effect on the water table as most of the abstracted water is derived from aquifer storage (contains no river source water anymore). Both the tracer plume and ground water table show less sensitivity to the well depth, compared to the pumping rate and well distance from river (Figs. 11 and 12). Only when the well is very close to the river does the flux area increase with the deeper well depth (Fig. 11c). If the well is located close to the river, this will limit the spatial extent of river water incursion and spread because the pumping will induce flow from the river towards the well (Fig. 11b).

The data for 2014 was analyzed to check the sensitivity of plume area and drawdown in pre- and post-monsoon to the different factors. For the infiltrated tracer plume area, the pumping rate is always the dominant parameter for the whole year (Fig. 12a). The Sobol sensitivity indices are slightly higher during the pre-monsoon (January to June). As there is less rainfall during the pre-monsoon,
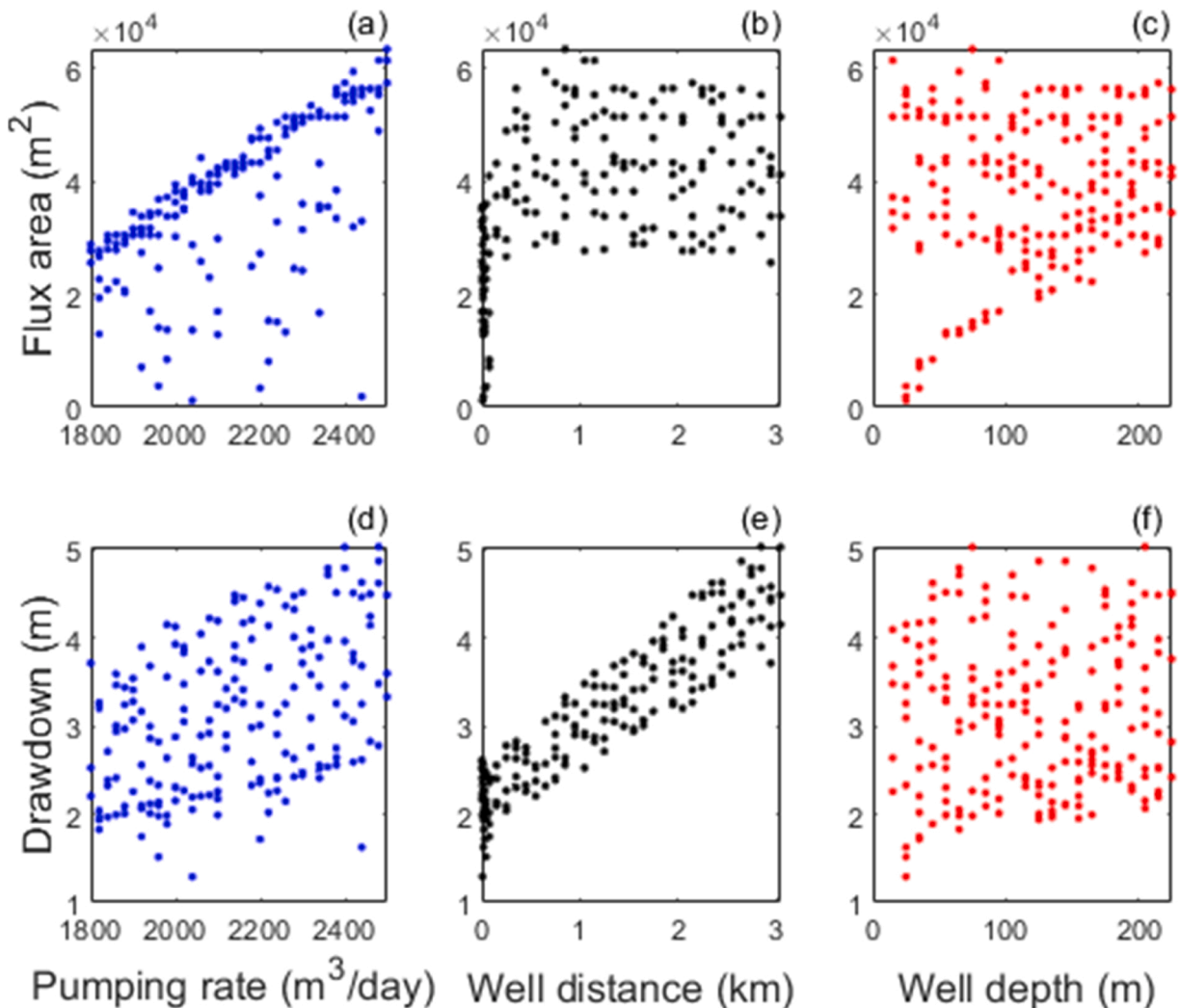
Fig. 11. Sensitivity analysis of modelled tracer plume area (a, b and c) and water drawdown at 25 km from river (d, e and f) as a function of pumping rate (a, d), well distance to the river (b, e) and well depth (c, f) for August 31, 2014.

the increase of pumping rate will cause more river water infiltration, thus increasing the tracer plume area. Higher pumping rates for municipal wells are commonly used in Patna to meet demands of increasing population and industrial usage. However, as the river water infiltration and groundwater table are sensitive to pumping rates, potential implementation of new wells and/or increasing pumping rates must be carefully considered, especially in pre-monsoon time. The plume area is relatively less sensitive to the pumping rate in monsoon and post-monsoon seasons (July to December). In contrast, the well distance is a secondary dominant parameter for plume area all the time, and the plume area is relatively more sensitive to the well distance in the monsoon and post-monsoon. The plume area is not sensitive to the well depth, even in July when the rainfall is heavy (Fig. 12a).

Well distance is the dominant parameter for water drawdown at 25 km for the whole year, and pumping rate the second-most dominant parameter (Fig. 12b). Water drawdown shows a similar sensitivity pattern in pre- and post-monsoon seasons.

Based on the 200 simulation results, triangulation-based cubic interpolation was used to interpolate more data points to analyze the relationship between the controlling factors and water drawdown and tracer concentration in the test well. With this analysis, the confidence level of well location and pumping rate characteristics can be estimated for water resource protection. When the pumping rate is high and the well distance is far away from the river, the water drawdown (at 25 km) is relatively high (Fig. 13a, c and Fig. S4). The drawdown shows a quasi-linear positive relationship with the pumping rate and the well distance from the river (Fig. 13a). This indicates that the pumping rate and location of new planned wells must be limited and optimized for the purpose of water resource protection. CGWB (2015) also showed that a modelled 12 m groundwater drawdown was reached in the highly urbanized part of Patna for even just a 2% increase in annual groundwater withdraw. Therefore, the groundwater table is very sensitive to the rate of well water abstraction as the precipitation is the major source term for the groundwater in Patna area.

When the pumping well is near to the river (< 500 m), there is a high possibility for the pumped water to contain water from the
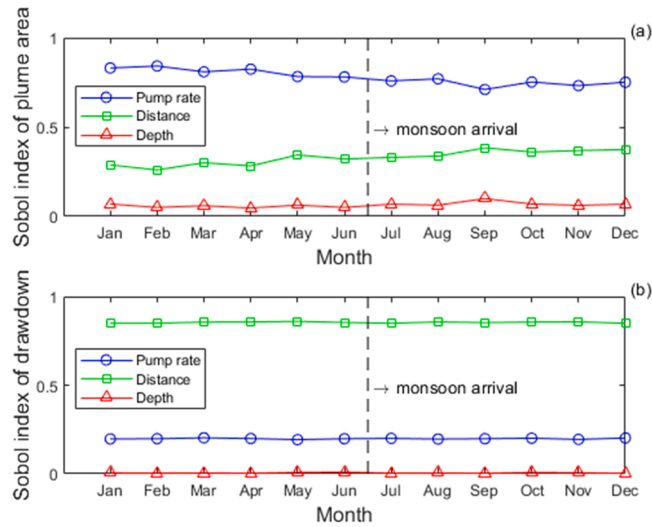
Fig. 12. Sobol sensitivity index (relative index: 1 means highest sensitivity and 0 indicates no sensitivity) for (a) tracer plume area and (b) drawdown of groundwater table at 25 km from the river related to the sensitivity factors (pump rate: 1800 – 2500 m³/day; well distance from the river: 2 – 3000 m; and well depth in the aquifer: 15 – 225 m) at year 2014.
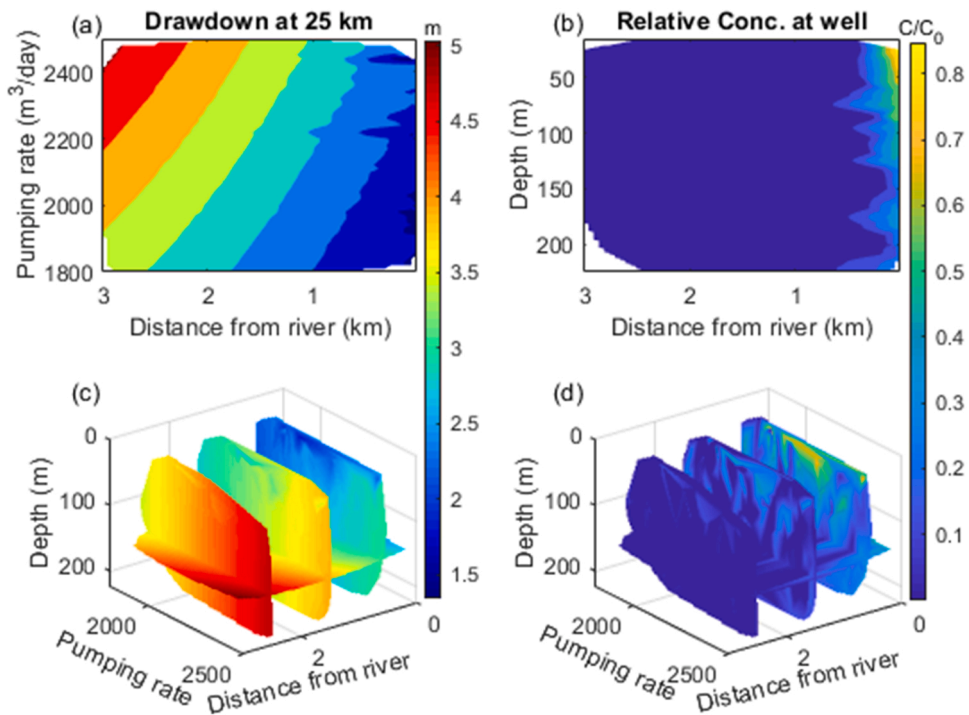

Fig. 13. Modelled groundwater drawdown distribution (a, c) related to the affecting factors at location 25 km from river on August 31, 2014. (a): drawdown (mean of data with different depth) related to pumping rate and distance; (c): drawdown related to the three factors. The tracer concentration (C/C₀) in the pumping well (b, d) related to the sensitivity factors on August 31, 2014. (b): Relative concentration (mean of data with different pumping rate) related to depth and distance; (d): concentration related to the three factors.

river (C/C₀ up to a maximum of 0.8). For locations greater than 1 km distance from the river, there is almost no river source water in the pumping well (C/C₀ < 0.1; Fig. 13b, d and Fig. S5). Generally, the pumped water contains more water from the river when the well depth is relatively shallow. The relative tracer concentration in the pumped water is less than 0.2 if the well depth is deeper than 200 m. However, it will be more than 0.5 if the depth is shallower than 150 m (when the well is located close to the river). The effect of pumping rate on the portion of river source water in pumped water is not substantial for the range of pumping rates considered

(Fig. 13d and Fig. S5). Therefore, the simulation results suggest that deep pumping wells at a distance greater than 1 km from the river could supply water less impacted by river water, and hence of higher quality, although importantly only to the extent that is determined by the proportion of river water in the produced water. Other factors, including local pollutant sources and in-aquifer geogenic biogeochemical contamination processes (Islam et al., 2004) might also affect the produced water quality.

4. Conclusions

For the majority of the year, groundwater under Patna flows from the aquifer into the River Ganges. River water starts infiltrating into the aquifer when the monsoon season starts. On average, the Ganges River becomes a source term for the groundwater for just 9% of the year (around 33 days with range 0 – 68 days) for the selected cross section. Installing new pumping water supply wells will result in more river water being transported into the aquifer. With a new implemented municipal purpose pumping well (pumping rate 2000 m^3/day), the time of river water infiltration increases to 68% of the year (around 253 days with range 140 − 365 days). A global sensitivity analysis shows that well pumping rate is the dominant factor controlling river plume extent, and that distance of the pumping well from the river is the second-most important factor. The horizontal location of well plays an important role for changes in groundwater table at a given location. The sensitivity of water drawdown shows a near-linear positive relation with the pumping rate and well distance from the river. Abstracted groundwater is expected to contain < 10% river water when wells are located > 1 km from the river.

The results suggest that uncertainty quantification of aquifer-river water exchange under transient conditions with pumping water should be conducted before installing municipal pumping wells or high pumping rate irrigation wells. The location of wells, their depth and pumping rate should be optimized to protect groundwater levels and to prevent contaminants being transported from the river to the abstracted groundwater.

In this study, we present a first-generation water exchange profile approach that can provide valuable input to models and related risk-assessment studies, water resources management and the biogeochemical analysis in the aquifer. It provides a system of research workflow for the assessment of water exchange trends between rivers and aquifers in other pumping impacted sites along Ganges. In future, a three-dimensional aquifer model with heterogeneous aquifer parameters and multiple wells considering variable pump rates and pump times may be necessary to provide more robust assessments of groundwater-river exchange along the Ganges.

CRediT authorship contribution statement

Chuanhe Lu: Conceptualization, Methodology, Formal analysis, Writing – original draft, Writing – review & editing, Visualization **Laura A. Richards:** Conceptualization, Methodology, Resources, Writing – review & editing **George J.L. Wilson:** Conceptualization, Methodology, Writing – review & editing, **Stefan Krause:** Conceptualization, Methodology, Writing – review & editing **Dan J. Lapworth:** Conceptualization, Methodology, Writing – review & editing **Daren C. Gooddy:** Conceptualization, Methodology, Writing – review & editing **Biswajit Chakravorty:** Conceptualization, Methodology, Writing – review & editing **David A. Polya:** Conceptualization, Methodology, Writing – review & editing, Resources, Supervision, Project administration, Funding acquisition **Vahid J. Niasar:** Conceptualization, Methodology, Writing – review & editing, Resources, Supervision.

Declaration of Competing Interest

The authors declare that they have no known competing financial interests or personal relationships that could have appeared to influence the work reported in this paper.

Data Availability

The precipitation data used in this study is available through Worldweatheronline (2021). The water level of Ganges River is available through Coss et al. (2020). The data of aquifer properties is available through CGWB (2015). The software PSUADE (version 1.7) used for sensitivity analysis is available via https://computing.llnl.gov/projects/psuade/software.

Acknowledgments

Appendix A. Supporting information

Supplementary data associated with this article can be found in the online version at doi:10.1016/j.ejrh.2022.101133.

References

Alakshendra, A., 2019. City profile: Patna, India. Environ. Urban. ASIA 10 (2), 374–392. https://doi.org/10.1177/0975425319859132.

Ascott, M.J., Bloomfield, J.P., Karapanos, I., Jackson, C.R., Ward, R.S., McBride, A.B., Dobson, B., Kieboom, N., Holman, I.P., Van Loon, A.F., Crane, E.J., Brauns, B., Rodriguez-Yebra, A., Upton, K.A., 2021. Managing groundwater supplies subject to drought: perspectives on current status and future priorities from England (UK). Hydrogeol. J. 29, 921–924. https://doi.org/10.1007/s10040-020-02249-0.

Ascott, M.J., Lapworth, D.J., Gooddy, D.C., Sage, R.C., Karapanos, I., 2016. Impacts of extreme flooding on riverbank filtration water quality. Sci. Total Environ. 554, 89–101. https://doi.org/10.1016/j.scitotenv.2016.02.169.

Battin, T.J., Kaplan, L.A., Findlay, S., Hopkinson, C.S., Marti, E., Packman, A.I., Newbold, J.D., Sabater, F., 2008. Biophysical controls on organic carbon fluxes in fluvial networks. Nat. Geosci. 1 (2), 95–100. https://doi.org/10.1038/ngeo101.

Bedekar, V., Morway, E.D., Langevin, C.D., Tonkin, M., 2016. MT3D-USGS version 1: A U.S. Geological Survey release of MT3DMS updated with new and expanded transport capabilities for use with MODFLOW: U.S. Geological Survey Techniques and Methods 6-A53, 69 p. https://doi.org/10.3133/tm6A53.

Boano, F., Packman, A.I., Cortis, A., Revelli, R., Ridolfi, L., 2007. A continuous time random walk approach to the stream transport of solutes. Water Resour. Res. 43 (10) https://doi.org/10.1029/2007WR006062.

Boano, F., Demaria, A., Revelli, R., Ridolfi, L., 2010. Biogeochemical zonation due to intrameander hyporheic flow. Water Resour. Res. 46 (2) https://doi.org/10.1029/2008WR007583.

Boano, F., Revelli, R., Ridolfi, L., 2013. Modeling hyporheic exchange with unsteady stream discharge and bedform dynamics. Water Resour. Res. 49 (7), 4089–4099. https://doi.org/10.1002/wrcr.20322.

Boano, F., Harvey, J.W., Marion, A., Packman, A.I., Revelli, R., Ridolfi, L., Wörman, A., 2014. Hyporheic flow and transport processes: mechanisms, models, and biogeochemical implications. Rev. Geophys. 52 (4), 603–679. https://doi.org/10.1002/2012RG000417.

Brikowski, T.H., Neku, A., Shrestha, S.D., Smith, L.S., 2014. Hydrologic control of temporal variability in groundwater arsenic on the Ganges floodplain of Nepal. Water Resour. Res. 518 (PC), 342–353. https://doi.org/10.1016/j.jhydrol.2013.09.021.

Cardenas, M.B., 2009a. A model for lateral hyporheic flow based on valley slope and channel sinuosity. Water Resour. Res. 45 (1) https://doi.org/10.1029/2008WR007442.

Cardenas, M.B., 2009b. Stream-aquifer interactions and hyporheic exchange in gaining and losing sinuous streams. Water Resour. Res. 45 (6) https://doi.org/10.1029/2008WR007651.

Central Ground Water Board (CGWB), Ministry of water resources, river development & Ganga rejuvenation, Goverment of India, Mid-eastern region, PATNA, 2015. Pilot project on aquifer mapping in Maner-Khagaul area, Patna district, Bihar (Watershed -GNDK013). Report. ⟨https://www.scribd.com/document/352363216/Patna-District-Bihar-Final⟩.

Cardenas, M.B., Wilson, J.L., Zlotnik, V.A., 2004. Impact of heterogeneity, bed forms, and stream curvature on subchannel hyporheic exchange. Water Resour. Res. 40 (8) https://doi.org/10.1029/2004WR003008.

Charlet, L., Polya, D.A., 2006. Arsenic in shallow, reducing groundwaters in southern Asia: an environmental health disaster. Elements 2, 91–96. https://doi.org/10.2113/gselements.2.2.91.

Chatterjee, R., Samadder, S., Mondal, D., Adhikari, K., 2020. Analysis of spatio-temporal trend in groundwater elevation data from arsenic affected alluvial aquifers – case study from Murshidabad district, West Bengal, Eastern India. J. Earth Syst. Sci. 129 (228) https://doi.org/10.1007/s12040-020-01489-8.

Chiang, W.-H., Kinzelbach, W., 2003. 3D-Groundwater Modeling with PMWIN. 3D-Groundwater Modeling with PMWIN. Springer, Berlin Heidelberg. https://doi.org/10.1007/978-3-662-05549-6.

Chow, R., Bennett, J., Dugge, J., Wöhling, T., Nowak, W., 2020. Evaluating subsurface parameterization to simulate hyporheic exchange: the Steinlach River test site. Groundwater 58 (1), 93–109. https://doi.org/10.1111/gwat.12884.

Coss, S., Durand, M., Yi, Y., Jia, Y., Guo, Q., Tuozzolo, S., Allen, G., Calmant, S., Pavelsky, T., 2020. Global river radar altimetry time series (GRRATS): new river elevation earth science data records for the hydrologic community. Earth Syst. Sci. Data 137–150. https://doi.org/10.5194/essd-12-137-2020.

Das, P., Mukherjee, A., Hussain, S.A., Jamal, S., Das, K., Shaw, A., Layek, M.K., Sengupta, P., 2021a. Stable isotope dynamics of groundwater interactions with Ganges river. Hydrol. Process. 35 (1) https://doi.org/10.1002/hyp.14002.

Das, P., Mukherjee, A., Lapworth, D.J., Das, K., Bhaumik, S., Layek, M., Shaw, A., Smith, M., Sengupta, P., MacDonald, A.M., Sen, J., 2021b. Quantifying the dynamics of sub-daily to seasonal hydrological interactions of Ganges river with groundwater in a densely populated city: Implications to vulnerability of drinking water sources. J. Environ. Manag. 288. https://doi.org/10.1016/j.jenvman.2021.112384.

Duttagupta, S., Mukherjee, A., Bhanja, S.N., Chattopadhyay, S., Sarkar, S., Das, K., Chakraborty, S., Mondal, D., 2020. Achieving sustainable development goal for clean water in India: influence of natural and anthropogenic factors on groundwater microbial pollution. Environ. Manag. 66 (5), 742–755. https://doi.org/10.1007/s00267-020-01358-6.

Goldschneider, A.A., Haralampides, K.A., MacQuarrie, K.T.B., 2007. River sediment and flow characteristics near a bank filtration water supply: implications for riverbed clogging. J. Hydrol. 344 (1–2), 55–69. https://doi.org/10.1016/j.jhydrol.2007.06.031.

Gomez-Velez, J.D., Harvey, J.W., 2014. A hydrogeomorphic river network model predicts where and why hyporheic exchange is important in large basins. Geophys. Res. Lett. 41 (18), 6403–6412. https://doi.org/10.1002/2014GL061099.

Gomez-Velez, J.D., Wilson, J.L., Cardenas, M.B., 2012. Residence time distributions in sinuosity-driven hyporheic zones and their biogeochemical effects. Water Resour. Res. 48 (9) https://doi.org/10.1029/2012WR012180.

Gomez-Velez, J.D., Wilson, J.L., Cardenas, M.B., Harvey, J.W., 2017. Flow and residence times of dynamic river bank storage and sinuosity-driven hyporheic exchange. Water Resour. Res. 53 (10), 8572–8595. https://doi.org/10.1002/2017WR021362.

de Graaf, I.E.M., Gleeson, T., (Rens) van Beek, L.P.H., Sutanudjaja, E.H., Bierkens, M.F.P., 2019. Environmental flow limits to global groundwater pumping. Nature 574 (7776), 90–94. https://doi.org/10.1038/s41586-019-1594-4.

Hubbs, S.A., 2006. Evaluating streambed forces impacting the capacity of riverbed filtration systems. In: Hubbs, S.A. (Ed.), Riverbank Filtration Hydrology. Nato Science Series: IV: Earth and Environmental Sciences, 60. Springer, Dordrecht. https://doi.org/10.1007/978-1-4020-3938-6_2.

Hughes, J.D., Langevin, C.D., Banta, E.R., 2017. Documentation for the MODFLOW 6 framework: U.S. Geological Survey Techniques and Methods, book 6, chap. A57, 40 p., https://doi.org/10.3133/tm6A57.

Islam, F.S., Gault, A.G., Boothman, C., Polya, D.A., Charnock, J.M., Chatterjee, D., Lloyd, J.R., 2004. Role of metal reducing bacteria in arsenic release in Bengal delta sediments. Nature 430, 68–71. https://doi.org/10.1038/nature02638.

Jasechko, S., Seybold, H., Perrone, D., Fan, Y., Kirchner, J.W., 2021. Widespread potential loss of streamflow into underlying aquifers across the USA. Nature 591, 391–395. https://doi.org/10.1038/s41586-021-03311-x.

Joekar-Niasar, V., Ataie-Ashtiani, B., 2009. Assessment of nitrate contamination in unsaturated zone of urban areas: the case study of Tehran, Iran. Environ. Geol. 57, 1785–1798. https://doi.org/10.1007/s00254-008-1464-0.

Johannesson, K.H., Yang, N., Trahan, A.S., Telfeyan, K., Jade Mohajerin, T., Adebayo, S.B., Akintomide, O.A., Chevis, D.A., Datta, S., White, C.D., 2019. Biogeochemical and reactive transport modeling of arsenic in groundwaters from the Mississippi River delta plain: An analog for the As-affected aquifers of South and Southeast Asia. Geochim. Cosmochim. Acta 264, 245–272. https://doi.org/10.1016/j.gca.2019.07.032.

Kiel, B.A., Cardenas, M.B., 2014. Lateral hyporheic exchange throughout the Mississippi River network. Nat. Geosci. 7 (6), 413–417. https://doi.org/10.1038/ngeo2157.

Krause, S., Hannah, D.M., Fleckenstein, J.H., Heppell, C.M., Pickup, R., Pinay, G., Robertson, A.L., Wood, P.J., 2011. Inter-disciplinary perspectives on processes in the hyporheic zone. Ecohydrology 4 (4), 481–499. https://doi.org/10.1002/eco.176.

Kumar, A., Anand, S., Kumar, M., Chandra, R., 2017. Groundwater assessment: a case study in Patna and Gaya district of Bihar. Int. J. Curr. Microbiol. Appl. Sci. 6 (12), 184–195. https://doi.org/10.20546/ijcmas.2017.612.024.

Lapworth, D.J., Dochartaigh, Ó., Nair, B., O'Keeffe, T., Krishan, J., MacDonald, G., Khan, A.M., Kelkar, M., Choudhary, N., Krishnaswamy, S., Jackson, C.R, J., 2021. Characterising groundwater-surface water connectivity in the lower Gandak catchment, a barrage regulated biodiversity hotspot in the mid-Gangetic basin. J. Hydrol. 594. https://doi.org/10.1016/j.jhydrol.2020.125923.

Magliozzi, C., Grabowski, R., Packman, A.I., Krause, S., 2018. Toward a conceptual framework of hyporheic exchange across spatial scales. Hydrol. Earth Syst. Sci. 22, 6163–6185. https://doi.org/10.5194/hess-2018-268.

Marion, A., Packman, A.I., Zaramella, M., Bottacin-Busolin, A., 2008. Hyporheic flows in stratified beds. Water Resour. Res. 44 (9) https://doi.org/10.1029/2007WR006079.

Marzadri, A., Tonina, D., Bellin, A., Valli, A., 2016. Mixing interfaces, fluxes, residence times and redox conditions of the hyporheic zones induced by dune-like bedforms and ambient groundwater flow. Adv. Water Resour. 88, 139–151. https://doi.org/10.1016/j.advwatres.2015.12.014.

Mehmood, T., Miller, G.R., Knappett, P.S.K., 2022. Testing alternative conceptual models of river-aquifer connectivity and their impacts on baseflow and river recharge processes. Hydrol. Process. 36 (3), e14545 https://doi.org/10.1002/hyp.14545.

Mukherjee, A., Bhanja, S.N., Wada, Y., 2018. Groundwater depletion causing reduction of baseflow triggering Ganges river summer drying. Sci. Rep. 8 (1), 1–9. https://doi.org/10.1038/s41598-018-30246-7.

Mulholland, P.J., Helton, A.M., Poole, G.C., Hall, R.O., Hamilton, S.K., Peterson, B.J., Tank, J.L., Ashkenas, L.R., Cooper, L.W., Dahm, C.N., Dodds, W.K., Findlay, S.E. G., Gregory, S.V., Grimm, N.B., Johnson, S.L., McDowell, W.H., Meyer, J.L., Valett, H.M., Webster, J.R., Thomas, S.M., 2008. Stream denitrification across biomes and its response to anthropogenic nitrate loading. Nature 452 (7184), 202–205. https://doi.org/10.1038/nature06686.

Munz, M., Krause, S., Tecklenburg, C., Binley, A., 2011. Reducing monitoring gaps at the aquifer-river interface by modelling groundwater-surface water exchange flow patterns. Hydrol. Process. 25 (23), 3547–3562. https://doi.org/10.1002/hyp.8080.

Ravenscroft, P., Brammer, H., Richards, K., 2009. Arsenic Pollution - A Global Synthesis. In: Royal Geographical Society with IBG, 588. Wiley-Blackwell, Chichester.

Ray, C., Melin, G., Linsky, R.B., 2003. Riverbank filtration: improving source-water quality. In: Water Science and Technology Library, 43. Kluwer Academic Publishers, Dordrecht, p. 364.

Richards, L.A., Kumar, A., Shankar, P., Gaurav, A., Ghosh, A., Polya, D.A., 2021. Distribution and geochemical controls of arsenic and uranium in groundwater-derived drinking water in Bihar, India. Int. J. Environ. Res. Public Health 17 (7), 1–29. https://doi.org/10.3390/ijerph17072500.

Richards, L.A., Kumari, R., Parashar, N., Kumar, A., Lu, C., Wilson, G., Lapworth, D., Niasar, V.J., Ghosh, A., Chakravorty, B., Krause, S., Polya, D.A., Gooddy, D.C., 2022. Environmental tracers and groundwater residence time indicators reveal controls of arsenic accumulation rates beneath a rapidly developing urban area in Patna, India. J. Contam. Hydrol. (accepted).

Rizzo, C.B., Song, X., de Barros, F.P.J., Chen, X., 2020. Temporal flow variations interact with spatial physical heterogeneity to impact solute transport in managed river corridors. J. Contam. Hydrol. 235. https://doi.org/10.1016/j.jconhyd.2020.103713.

Rosenberry, D.O., Healy, R.W., 2012. Influence of a thin veneer of low-hydraulic-conductivity sediment on modelled exchange between river water and groundwater in response to induced infiltration. Hydrol. Process 26 (4), 544–557. https://doi.org/10.1002/hyp.8153.

Saha, D., Sinha, U.K., Dwivedi, S.N., 2011. Characterization of recharge processes in shallow and deeper aquifers using isotopic signatures and geochemical behavior of groundwater in an arsenic-enriched part of the Ganges Plain. Appl. Geochem. 26 (4), 432–443. https://doi.org/10.1016/j.apgeochem.2011.01.003.

Saha, D., Dwivedi, S.N., Singh, R.K., 2014. Aquifer system response to intensive pumping in urban areas of the Gangetic plains, India: the case study of Patna. Environ. Earth Sci. 71 (4), 1721–1735. https://doi.org/10.1007/s12665-013-2577-7.

Salehin, M., Packman, A.I., Paradis, M., 2004. Hyporheic exchange with heterogeneous streambeds: laboratory experiments and modeling. Water Resour. Res. 40 (11) https://doi.org/10.1029/2003WR002567.

Sandhu, C., Grischek, T., Schoenheinz, D., Prasad, T., Thakur, A.K., 2011. Evaluation of bank filtration for drinking water supply in Patna by the Ganga River, India. In: Shamrukh, M. (Ed.), Riverbank filtration for water security in desert Countries. NATO Science for Peace and Security Series C: Environmental Security. Springer, Dordrecht. https://doi.org/10.1007/978-94-007-0026-0_12.

Saunders, J.A., Lee, M.-K., Uddin, A., Mohammad, S., Wilkin, R.T., Fayek, M., Korte, N.E., 2005. Natural arsenic contamination of Holocene alluvial aquifers by linked tectonic, weathering, and microbial processes. Geochem. Geophys. Geosyst. 6 (4) https://doi.org/10.1029/2004GC000803.

Sawyer, A.H., Cardenas, M.B., 2009. Hyporheic flow and residence time distributions in heterogeneous cross-bedded sediment. Water Resour. Res. 45 (8) https://doi.org/10.1029/2008WR007632.

Schubert, J., 2006. Experience with riverbed clogging along the Rhine River. In: Hubbs, S.A. (Ed.), Riverbank Filtration Hydrology. Springer, Dordrecht, pp. 221–242.

Shamsuddha, M., Taylor, R.G., Ahmed, K.M., Zahid, A., 2011. The impact of intensive groundwater abstraction on recharge to a shallow regional aquifer system: evidence from Bangladesh. Hydrogeol. J. 19, 901–916. https://doi.org/10.1007/s10040-011-0723-4.

Singh, T., Gomez-Velez, J.D., Krause, S., 2020. Effects of successive peak-flow events on hyporheic exchange and residence times. Water Resour. Res. 56 (8) https://doi.org/10.1029/2020WR027113.

Singh, V., Raj, C., Chakraborty, B., 2018. River aquifer interaction in Lower Gandak Command Area in Bihar. India IOP Conf. Ser. Earth Environ. Sci. 150, 012003.

Smedley, P.L., Kinniburgh, D.G., 2002. A review of the source, behaviour and distribution of arsenic in natural waters. Appl. Geochem. 17 (5), 517–568. https://doi.org/10.1016/S0883-2927(02)00018-5.

Sobol, I.M., 2001. Global sensitivity indices for nonlinear mathematical models and their Monte Carlo estimates. Math. Comput. Simul. (1–3), 271–280. https://doi.org/10.1016/S0378-4754(00)00270-6.

Song, X., Chen, X., Zachara, J.M., Gomez-Velez, J.D., Shuai, P., Ren, H., Hammond, G.E., 2020. River dynamics control transit time distributions and biogeochemical reactions in a dam-regulated river corridor. Water Resour. Res. 56 (9) https://doi.org/10.1029/2019WR026470.

Stonedahl, S.H., Sawyer, A.H., Stonedahl, F., Reiter, C., Gibson, C., 2018. Effect of heterogeneous sediment distributions on hyporheic flow in physical and numerical models. Groundwater 56 (6), 934–946. https://doi.org/10.1111/gwat.12632.

Su, G.W., Jasperse, J., Seymour, D., Constantz, J., Zhou, Q., 2007. Analysis of pumping-induced unsaturated regions beneath a perennial river. Water Resour. Res. 43 (8) https://doi.org/10.1029/2006WR005389.

Tong, C., 2017. PSUADE short manual. Lawrence Livermore National Laboratory (LLNL), Livermore, CA, USA. ⟨https://computing.llnl.gov/projects/psuade/software⟩.

Trauth, N., Fleckenstein, J.H., 2017. Single discharge events increase reactive efficiency of the hyporheic zone. Water Resour. Res. 53 (1), 779–798. https://doi.org/10.1002/2016WR019488.

Trauth, N., Musolff, A., Knöller, K., Kaden, U.S., Keller, T., Werban, U., Fleckenstein, J.H., 2018. River water infiltration enhances denitrification efficiency in riparian groundwater. Water Res. 130, 185–199. https://doi.org/10.1016/j.watres.2017.11.058.

Ulrich, C., Hubbard, S.S., Florsheim, J., Rosenberry, D., Borglin, S., Trotta, M., Seymour, D., 2015. Riverbed clogging associated with a California riverbank filtration system: An assessment of mechanisms and monitoring approaches. J. Hydrol. 529 (3), 1740–1753. https://doi.org/10.1016/j.jhydrol.2015.08.012.

van Geen, A., Bostick, B.C., Thi Kim Trang, P., Lan, V.M., Mai, N.N., Manh, P.D., Viet, P.H., Radloff, K., Aziz, Z., Mey, J.L., Stahl, M.O., Harvey, C.F., Oates, P., Weinman, B., Stengel, C., Frei, F., Kipfer, R., Berg, M., 2013. Retardation of arsenic transport through a Pleistocene aquifer. Nature 501 (7466), 204–207. https://doi.org/10.1038/nature12444.

Vaux, W.G., 1968. Intragravel flow and interchange of water in a streambed. Fish. Bull. 66 (3), 479–489.

Vukovic, M., Soro, A., 1992. Determination of hydraulic conductivity of porous media from grain-size composition. Water Resources Publications, USA.

Wallis, I., Prommer, H., Berg, M., Siade, A.J., Sun, J., Kipfer, R., 2020. The river–groundwater interface as a hotspot for arsenic release. Nat. Geosci. 13 (4), 288–295. https://doi.org/10.1038/s41561-020-0557-6.

Ward, A.S., Schmadel, N.M., Wondzell, S.M., Gooseff, M.N., Singha, K., 2017. Dynamic hyporheic and riparian flow path geometry through base flow recession in two headwater mountain stream corridors. Water Resour. Res. 53 (5), 3988–4003. https://doi.org/10.1002/2016WR019875.

Worldweatheronline (2021). ⟨www.worldweatheronline.com⟩. Accessed January 2021.

Wörman, A., Packman, A.I., Marklund, L., Harvey, J.W., Stone, S.H., 2007. Fractal topography and subsurface water flows from fluvial bedforms to the continental shield. Geophys. Res. Lett. 34 (7), L07402 https://doi.org/10.1029/2007GL029426.

Wroblicky, G.J., Campana, M.E., Valett, H.M., Dahm, C.N., 1998. Seasonal variation in surface-subsurface water exchange and lateral hyporheic area of two stream-aquifer systems. Water Resour. Res. 34 (3), 317–328. https://doi.org/10.1029/97WR03285.

Wu, L., Singh, T., Gomez-Velez, J., Nützmann, G., Wörman, A., Krause, S., Lewandowski, J., 2018. Impact of dynamically changing discharge on hyporheic exchange processes under gaining and losing groundwater conditions. Water Resour. Res. 54 (12) https://doi.org/10.1029/2018WR023185.

Wu, L., Gomez-Velez, J.D., Krause, S., Wörman, A., Singh, T., Nützmann, G., Lewandowski, J., 2020. How does daily groundwater table drawdown affect the diel rhythm of hyporheic exchange? Hydrol. Earth Syst. Sci. https://doi.org/10.5194/hess-2020-288.

Zhang, J., Song, J., Long, Y., Zhang, Y., Zhang, B., Wang, Y., Wang, Y., 2017. Quantifying the spatial variations of hyporheic water exchange at catchment scale using the thermal method: a case study in the Weihe River, China. Adv. Meteorol. 2017 https://doi.org/10.1155/2017/6159325.

Zhang, Y., Hubbard, S., Finsterle, S., 2011. Factors governing sustainable groundwater pumping near a river. Ground Water 49 (3), 432–444. https://doi.org/10.1111/j.1745-6584.2010.00743.x.